Hindawi
Advances in Civil Engineering
Volume 2020, Article ID 9568279, 11 pages
https://doi.org/10.1155/2020/9568279

Research Article

Influence of Underpinning Pile Drilling Construction on the Bearing Behavior of Existing Loaded Foundation Piles: Case Study

Hua-feng Shan,[1,2,3] **Tang-dai Xia**,[2] **Feng Yu**,[4] **Hai-bing Tao**,[3] **and Shao-heng He**[2]

[1]*School of Civil Engineering and Architecture, Taizhou University, Taizhou 318000, China*
[2]*Research Center of Coastal and Urban Geotechnical Engineering, Zhejiang University, Hangzhou 310058, China*
[3]*Fangyuan Construction Group Co., Ltd., Taizhou 318000, China*
[4]*School of Civil Engineering and Architecture, Zhejiang Sci-Tech University, Hangzhou 310018, China*

Correspondence should be addressed to Hua-feng Shan; shanhf@zju.edu.cn

Received 29 October 2019; Accepted 21 February 2020; Published 19 March 2020

Academic Editor: Giosuè Boscato

The mechanism of drilling borehole and its influence on the bearing behavior of existing foundation piles are unclear, hindering the application of excavation techniques. This paper proposes a new excavation scheme for high-rise buildings in downtown and develops theoretical formulas to calculate the skin friction and end resistance of existing foundation piles affected by adjacent borehole drilling for installing underpinning piles. These underpinning piles are installed and connected with the existing pile by the head cap before excavation. In a case study, the parameter analysis was then performed to understand the effect of underpinning construction on the bearing behavior of existing foundation piles in terms of skin friction and end resistance. The results show that borehole diameter, depth of drilling borehole, distance between the existing foundation pile and drilling borehole, and number of boreholes have a negligible influence on the end resistance of existing foundation piles. The effect of drilling parameters on the skin friction of existing foundation pile, as well as the influence extent, varies for different parameters. The depth of drilling borehole and the number of boreholes have significant influence and thus should be considered in real engineering design while the borehole diameter and the pile-pile distance have a negligible effect. The proposed new excavation technique could be potentially adopted for real engineering design of underneath excavation projects for high-rise buildings in downtown.

1. Introduction

As economies develop and urban populations rise, developers must meet the rapidly increasing demand for housing and, especially, the parking market. One way is to replace older buildings that have limited parking facilities with new structures with sufficient parking capacity, which is economically inefficient [1].

A more economical means to add parking spaces to existing buildings is retrofitting, for example, excavation beneath existing buildings. Qiu et al. [2] reported the structural design for renovation and extension of Beijing Music Hall. The corresponding techniques are challenging and still immature as limited applications of these techniques in fields have been reported. Wen et al. [3] proposed the deformation control techniques for excavation beneath existing buildings. Simpson and Vardanega [4] and Shan et al. [5] monitored the whole construction process of British Library excavation and the No. 3 subsection of Ganshuixiang Construction Project, respectively.

The excavation beneath existing buildings, particularly high-rise buildings, inevitably causes the ground stress field, which leads to the stress change at the pile-soil surface and the pile end, thereby reducing the pile bearing capacity and integrity of the piled foundation. Given that the bearing capacity of piles after excavation fails to be practically measured in field, it is of great importance to conduct theoretical and numerical analysis to estimate its bearing capacity after excavation and the detrimental effects of excavation-induced soil movement on adjacent existing pile foundation, particularly during the engineering design stage.

The influence of excavation on an adjacent single pile in different types of formation (e.g., soft clay and sand) has been investigated by several researchers [6–10]. These studies generally show that bending moment and deflection occur, and pile head boundary condition and embedded depth of the wall, as well as formation level of the excavation, play an important role in influencing the pile response due to an adjacent excavation. As piles are often used in groups, researchers are also interested in exploring the influence of excavation on a pile within a pile group [11–13]. Generally, their results show that the interaction effect between piles depends on the arrangement of piles (e.g., either piles are arranged in a row parallel to the retaining wall or in a line perpendicular to the wall), pile spacing, pile number, and whether piles are capped-head or free-head ones. The excavation-induced bending decreases with the number of piles. The interior piles of the pile group experience lower bending moments than those of peripheral piles.

In practice, the applications of excavation techniques are under development, particularly for high-rise buildings in downtown, where limited construction space is allowed in most countries. In this study, a new excavation technique was proposed and its application was simulated in a real project. For this excavation scenario, the underpinning piles were installed and connected with the existing pile by the head cap before excavation. To understand the influence of drilling construction of underpinning piles on the bearing behavior of existing piles, this paper studies the influence of underpinning pile drilling construction on bearing behavior of foundation piles in a case study. Our results indicate that it is promising for designers to utilize the proposed excavation technique in future engineering projects.

1.1. Excavation Scheme. Figure 1 illustrates the construction process for adding extra space beneath the existing building. The whole process includes five steps, and they are described as follows:

(1) The retaining structure (wall) is installed to support the excavation, as shown in Figure 1(a).

(2) As the bearing capacity of existing piles decreases with the excavation depth, the settlement of existing buildings can occur; underpinning piles in groups are installed and connected with existing piles via the cap before the excavation, as shown in Figure 1(b).

(3) The soil is excavated layer by layer until the designed depth, and then bottom slabs of the new basement are cast, as shown in Figure 1(c).

(4) Pillars are cast at the specific location of the new basement. The pillar is prepared to support the superstructure, as shown in Figure 1(d).

(5) To maximize the space, the pile segments above the bottom slab of the new basement are cut and removed, as shown in Figure 1(e). After completing the above five steps, the main structure of the new basement is obtained. The corresponding stress analysis is then presented in the next section.

1.2. Calculation Model for Stress. Figure 2 shows the calculation model for the above pile structure during the drilling construction process.

The vertical effective stress before underpinning pile drilling construction σ_{vb} could be estimated using the following empirical equation:

$$\sigma_{vb} = \gamma' z + q, \tag{1}$$

where γ' is the effective unit weight of soil and q is the soil load caused by the load of superstructure.

The vertical effective stress after underpinning pile drilling construction σ_{va} is

$$\sigma_{va} = \gamma' z + q - \sigma_z, \tag{2}$$

where σ_z is the vertical effective stress at the calculation point.

The effective stress σ_z at the calculation point could be estimated by the Mindlin solution [14–16], as shown in Figure 3.

$$\sigma_z = \frac{p}{4\pi(1-\mu)}\left\{2(1-\mu)\left(\arctan^{-1}\frac{a}{z_1} + \arctan^{-1}\frac{a}{z_2}\right) + \frac{az_1}{r_1^2} + \frac{a[h+(3-4\mu)z]}{r_2^2} + \frac{4ahzz_2}{r_2^4}\right\}, \tag{3}$$

where μ is Poisson's ratio; a is the width of the strip load; h is the drilling depth; z is the depth of the calculation point; z_1, z_2, r_1, and r_2 are the calculation parameters, $z_1 = z - h$; $z_2 = z + h$; $r_1^2 = a_2 + z_1^2$; $r_2^2 = a^2 + z_2^2$; and p is the vertical effective stress at the borehole bottom of the underpinning pile. $p = \gamma' h$.

The effective stress σ_{zd} due to the underpinning pile drilling construction could be calculated by the following formula using the superposition principle, as shown in Figure 4:

$$\sigma_{zd} = \sigma_{z2} - \sigma_{z1}, \tag{4}$$

where σ_{z1} and σ_{z2} are the effective stresses caused by a_1 and a_2, respectively. It can be concluded from formula (3) that as long as the drilling depth, borehole diameter, and the distance between the borehole and the existing pile are determined, the effective stress of the soil at the calculation point is only related to its depth. Meanwhile, the excavation for installing underpinning piles should be conducted with carefulness to minimize the soil disturbance.

The bearing capacity of a pile can be assessed by its skin friction and end resistance, the formulas of which are then derived in the next two sections.

1.2.1. Skin Friction. In general, the distance between the underpinning pile and the existing foundation pile is small [17, 18]. Thus, the process of underpinning pile borehole may affect skin friction along the existing foundation pile.

According to the suggestions of Burland [19] and Loukidis and Salgado [20], the unit ultimate skin friction along the pile f_s can be written as

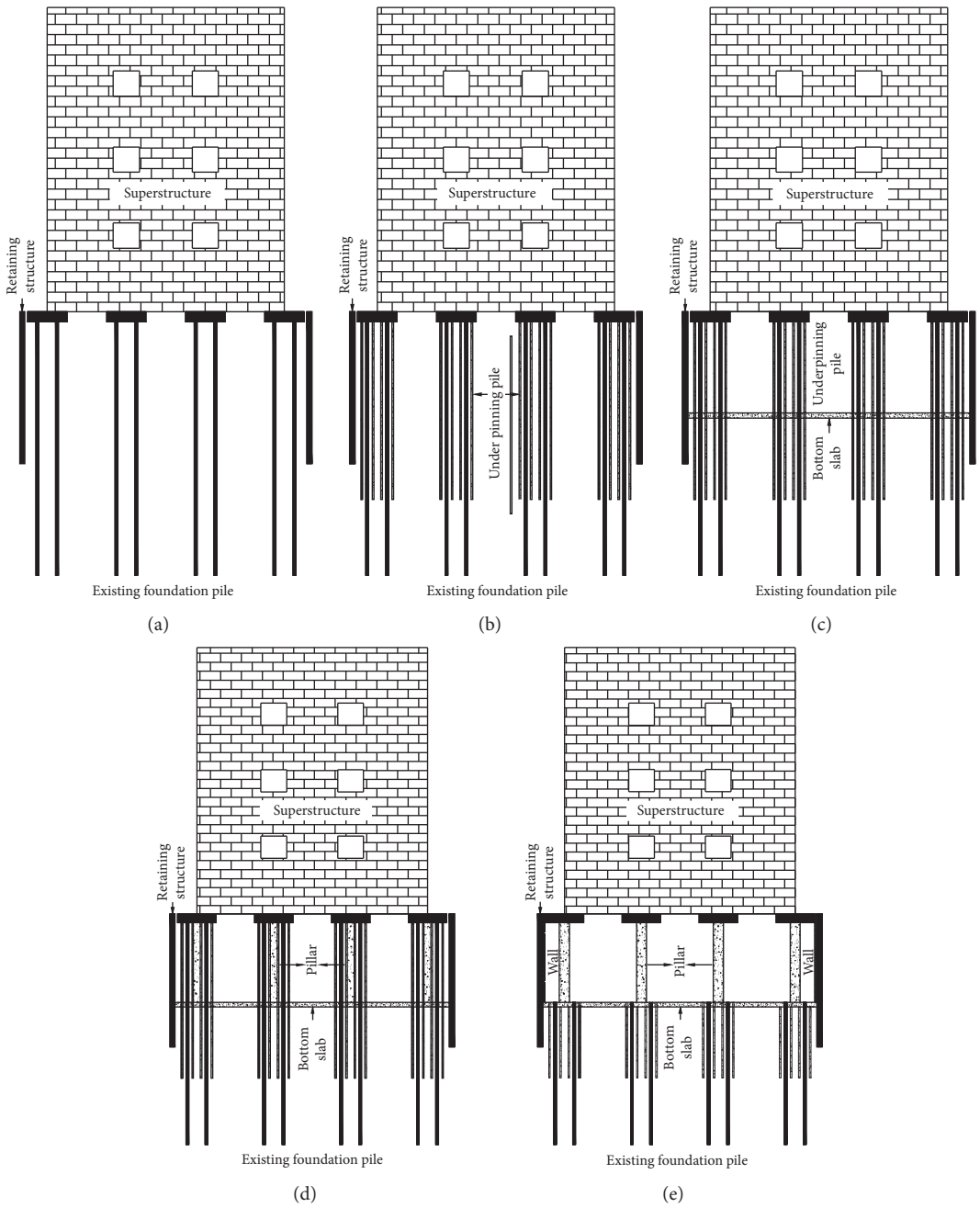

Figure 1: The sketch of the construction process for excavation beneath the existing building. (a) Retaining structure. (b) Underpinning pile. (c) Excavation. (d) Cast pillar. (e) Cutting pile.

$$f_s = K\sigma_v \tan\delta, \tag{5}$$

where K is the coefficient of lateral earth pressure; σ_v is the vertical effective stress; and δ is the angle of friction at existing foundation pile-soil interface. The product $K \tan\delta$ is sometimes denoted by β, and the use of $\beta\sigma_v$ to calculate f_s is known as the "β method" [21].

As for the coefficient of lateral earth pressure K, Zhang et al. [22] proposed the following expression:

$$K = 1.5(1 - \sin\varphi), \tag{6}$$

where φ is the internal friction angle.

Zhang et al. [23] suggested that the value of K for different pile-soil interactions is (0.7~4.0) K_0 based on the statistical data. Note that K_0 is the coefficient of earth pressure at rest. Generally, the pile-soil system has a long time for consolidation before the basement-supplementing retrofit engineering. Therefore, this paper assumes the soil around the pile is in the normal consolidation state [24]. The coefficient of lateral earth pressure K can be expressed as

$$K = 1 - \sin\varphi', \tag{7}$$

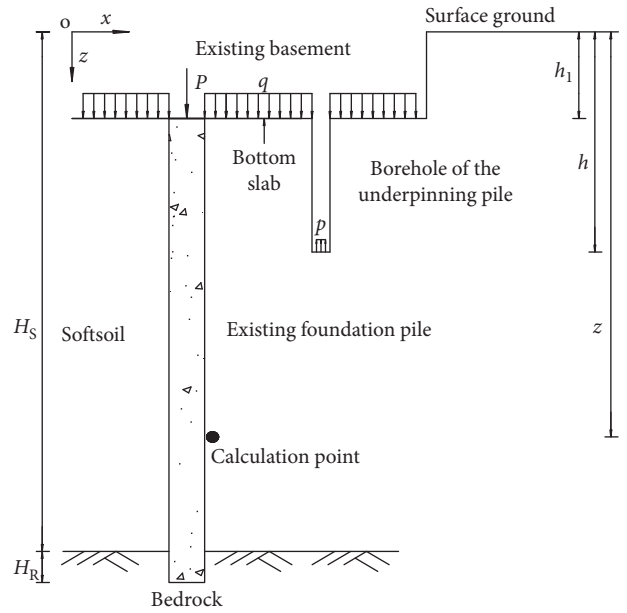

Figure 2: Calculation model of underpinning pile drilling construction.

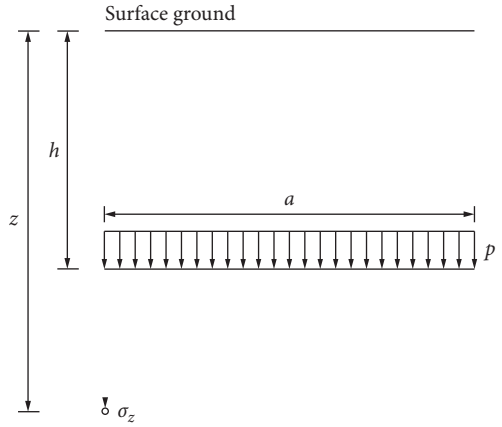

Figure 3: The sketch of Mindlin's stress solution.

where φ' is the effective internal friction angle.

The drilling construction of underpinning piles could be regarded as excavation, as shown in Figure 2. This would break the existing equilibrium state in the pile-soil system, which could not reach the new equilibrium timely. Consequently, the soil is in the state of overconsolidation. The coefficient of lateral earth pressure (K_{OCR}) is related to the overconsolidation ratio (OCR) [25]:

$$K_{OCR} = (1 - \sin\varphi')\mathrm{OCR}^{\sin\varphi'}. \tag{8}$$

It should be noted that the formula for K_{OCR} applies up to a limit of $K_p = (1 + \sin\varphi')/(1 - \sin\varphi')$. The overconsolidation ratio is defined as the ratio of vertical effective stress before underpinning pile drilling construction to that after the pile drilling construction.

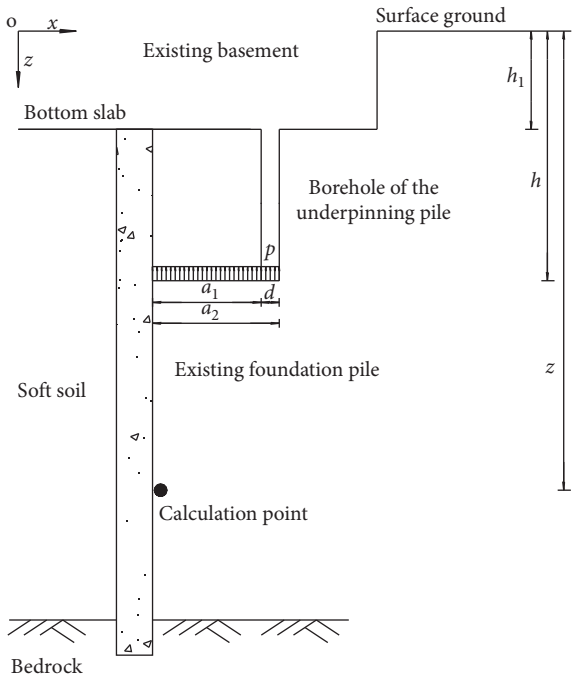

Figure 4: The sketch of the superposition principle.

$$\mathrm{OCR} = \frac{\sigma_{vb}}{\sigma_{va}}. \tag{9}$$

1.2.2. End Resistance. The Hoek–Brown criterion is shown in Figure 5, and its formula is as follows [26, 27]:

$$\frac{\sigma_1 - \sigma_3}{\sigma_c} = \sqrt{m\frac{\sigma_3}{\sigma_c} + s}, \tag{10}$$

where σ_1 and σ_3 are the major and minor failure stresses, respectively; σ_c is the compressive strength of the intact rock; and m and s are, respectively, the parameters of the Hoek–Brown criterion.

The strength modulus β and tensile strength coefficient of the rock mass ξ are

$$\beta = \frac{m\sigma_c}{8}, \tag{11}$$

$$\xi = \frac{8s}{m^2}, \tag{12}$$

where β and ξ are directly on the parameters m and s.

Lambe's variables (dimensionless) p and q could be expressed by the instantaneous angle of friction ρ.

$$p = \frac{\cot^2\rho}{2} - \xi, \tag{13}$$

$$q = \frac{1 - \sin\rho}{\sin\rho}. \tag{14}$$

The average overburden load in ground h_m (dimensionless) is [28]

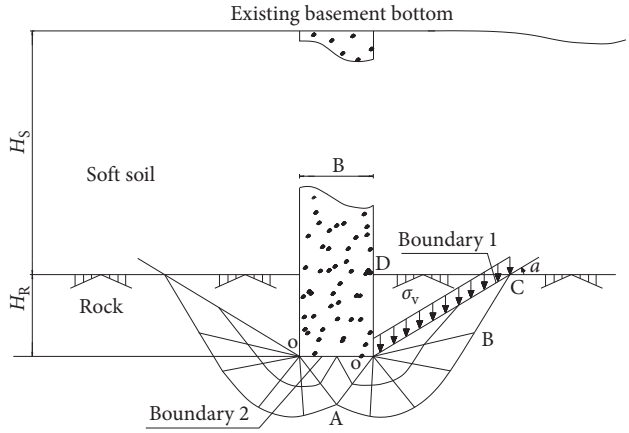

Figure 5: The sketch of pile tip failure.

$$h_m = \frac{H_s\gamma_s}{\beta} + \frac{H_R\gamma_R}{2\beta}, \tag{15}$$

where γ_s and γ_R are effective weights of the soil and the rock, respectively; H_s is the thickness of the soil; and H_R is the depth of the pile embedded into the rock.

The underpinning pile drilling construction would influence the ultimate bearing capacity at the tip pile. Before the underpinning pile drilling construction, the average overburden load in ground h_m is [29]

$$h_m = \frac{\gamma_R H_R}{2\beta} + \frac{\gamma_s H_s + p_c}{\beta}. \tag{16}$$

After the underpinning pile drilling construction, the average overburden load in ground h_m is

$$h_m = \frac{\gamma_R H_R}{2\beta} + \frac{\gamma_s H_s + p_c - \sigma_{hd}}{\beta}, \tag{17}$$

where σ_{hd} is the effective stress at the tip of the pile due to the underpinning pile drilling construction. It could be calculated by formula (4).

The vertical stress σ_v exerted upon boundary 1 is

$$\sigma_v = h_m \cos\alpha, \tag{18}$$

where α is the angle of inclination for the assumed virtual failure surface.

The stress component σ_v in the plane direction that represents boundary 1 (t_1) and the one that runs perpendicular to it (s_1) are as follows:

$$t_1 = \sigma_v \sin\alpha = h_m \sin\alpha\cos\alpha, \tag{19}$$

$$s_1 = \sigma_v \cos\alpha = h_m \cos^2\alpha. \tag{20}$$

The following formula holds for Mohr's circle at boundary 1 (see Figure 6):

$$(p_1 - s_1)^2 + t_1^2 = q_1^2, \tag{21}$$

where p_1 and q_1 are variables of Lambe that verify the Hoek–Brown criterion expressed by formulas (13)–(14), depending on the instantaneous angle of friction (ρ).

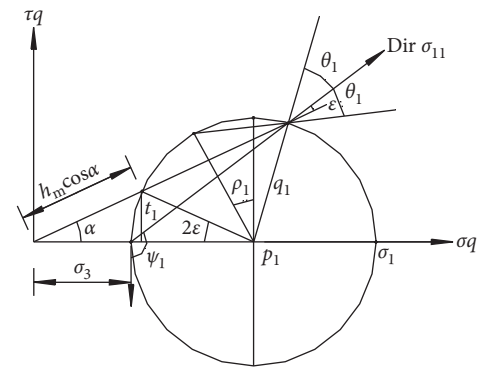

Figure 6: Mohr's circle for boundary 1.

Taken into formulas (19)–(20), the angle α for virtual boundary 1 is expressed as follows:

$$\cos\alpha = \frac{p_1^2 - q_1^2}{2p_1 h_m - h_m^2}. \tag{22}$$

The angle of inclination for the main major stress for boundary 1 regarding vertical axis ψ_1 is

$$\psi_1 = \frac{\pi}{2}\alpha + \varepsilon, \tag{23}$$

where ε is the angle that forms the main major stress with the inclination of the ground.

It can also be deduced from Figure 6 that angle ε is expressed by

$$\tan(2\varepsilon) = \frac{t_1}{(p_1 - s_1)}. \tag{24}$$

Given this, angle ε and angle ψ_1 can be expressed as a function of angle α and thus as a function of angle ρ_1 (ρ_1 is the instantaneous angle of internal friction for boundary 1) according to formula (22).

The angle θ_1 that forms the family of characteristic line 1 with the ground is

$$\theta_1 = \frac{\pi}{4} - \frac{\rho_1}{2}. \tag{25}$$

Riemann's invariant $I(\rho)$ is a function of ρ, as defined by the following formula:

$$I(\rho) = \frac{1}{2}\left[\cot\rho + \ln\cot\left(\frac{\rho}{2}\right)\right]. \tag{26}$$

Throughout the length of any characteristic line that surrounds the singular point O, the following relation could be verified [30]:

$$I(\rho) + \psi = \text{constant}. \tag{27}$$

This relationship enables one to transfer the stress state from boundary 1 to boundary 2 because

$$I(\rho_1) + \psi_1 = I(\rho_2) + \psi_2 = \text{constant}, \tag{28}$$

where ρ_2 and ψ_2 are the instantaneous angle of internal friction for boundary 2 and angle of inclination of the main major stress for boundary 2 (considering the vertical axis). The pile tip load is always vertical; therefore, $\psi_2 = 0$.

The embedment ratio n can be expressed by

$$n = \frac{H_R}{B} = \frac{\sin\alpha}{2}\frac{OC}{OM} = \frac{\sin\alpha}{2}\frac{OC}{OB}\frac{OB}{OA}\frac{OA}{OM}, \quad (29)$$

where B is the diameter of the pile.

The following formula could be expressed by the OBC triangle, OAB Prandtl's plastified radial zone, and OMA triangle:

$$n = \frac{\sin\alpha\cos\theta_1}{\sin(\theta_1+\varepsilon)}\sqrt{\frac{\tan\rho_1}{\tan\rho_2}}. \quad (30)$$

The above formula could be solved by iteration calculation.

The ultimate bearing capacity under two-dimensionality hypothesis σ_h^* is

$$\sigma_h^* = \beta(p_2+q_2) = \beta\left(\frac{\cot^2\rho_2}{2} + \frac{1-\sin\rho_2}{\sin\rho_2} - \xi\right). \quad (31)$$

Once the ultimate bearing capacity has been obtained under the plane strain hypothesis, it is necessary to take into account the three-dimensional geometry of the pile.

The shape factor S_β is

$$s_\beta = 1 + \tan\rho_m, \quad (32)$$

where ρ_m is an average angle of friction. It is established by the following formula:

$$\frac{2}{\sin\rho_m} = \frac{1}{\sin\rho_1} + \frac{1}{\sin\rho_2}. \quad (33)$$

The ultimate bearing capacity at the tip of the pile σ_{hp} is

$$\sigma_{hp} = s_\beta\sigma_h^*. \quad (34)$$

The ultimate bearing capacity at the tip of the pile during the pile drilling construction could be calculated by replacing formulas (16)–(17) with formula (15).

1.3. Case Study. A typical old building in downtown was selected as a prototype structure for excavation analysis. This old building, i.e., Zhejiang Hotel, was built in 1997 and open to the public in 1999. It is located in the Central Business District, Hangzhou downtown, China, as shown in Figure 7. The main building and the attached building of Zhejiang Hotel are 12 floors and four floors, respectively. There was one layer of the basement. The pile-raft foundation with a diameter from 0.6 m to 0.9 m was used. The pile was cast with the strength level of C30 (concrete strength grade in China) and its rock-socketed depth is more than 1.0 m. The building site is a typical soft soil area, and the mechanical parameters of soils are shown in Table 1. The groundwater table at this site was about 0.5 m below the ground surface. To calculate the end resistance of piles, for highly weathered andesite (Table 1) in our case study, m and s are 0.09 and 10^{-5}, respectively [31, 32]. Note m and s are, respectively, the parameters of the Hoek–Brown criterion (see formula (10)).

As Zhejiang Hotel is located in the most flourishing merchandise street, there is no available place for parking. The existing one layer of basement failed to meet the increasing parking requirements. Thus, the owner of Zhejiang Hotel decided to excavate another one layer of basement beneath the existing one. Then, the design basement would add an area of 2,800 m^2. The design of this excavation project is completed, but the engineering work has not started. The new excavation technique proposed in this paper is applied in this case project, followed by a parameter analysis regarding the influence of underpinning pile diameter, depth of drilling borehole, distance between the existing foundation pile and drilling borehole, and number of boreholes on the skin friction and end resistance of the existing pile during the underpinning pile construction.

1.4. Parameter Analysis and Discussion. According to the excavation design of the case project, the initial diameter, length, and rock-socketed depth of the existing foundation pile are 0.9 m, 34 m, and 1.1 m, respectively. The load applied at the head of the existing foundation pile is 4,330 kN. The buried depth of existing basement is 5.1 m. The formation layer along its depth is mucky silty clay, mucky clay, clay, silty clay, and clay, as shown in Figure 8.

1.4.1. Drilling Borehole Diameter. The influence of borehole diameter on the skin friction and end resistance of the existing foundation pile is analyzed in this section, and the results are shown in Figure 8 and Table 2. The depth of borehole is 17.5 m and space between existing foundation piles is 0.5 m. The influence of borehole diameter on the skin friction and end resistance of the existing pile was investigated by varying the borehole diameter from 0.26 m to 0.34 m while maintaining the other parameters constant. The above parameter values are input into formulas (5) to (9) to obtain the skin friction of the existing pile and input into formulas (10) to (34) to obtain the end resistance of the existing pile.

Figure 8 shows the influence of borehole diameter on the skin friction of the existing pile. The skin friction varies with different soil layers around the pile. It decreases slowly with an increase in the borehole diameter within the depth of borehole (17.5 m). This decrease reaches the maximum at the interfacial zone between mucky silty clay and mucky clay formation when the borehole diameter increases from 0.26 m to 0.34 m.

The drilling construction, similar to the excavation, could be regarded as the unloading of soil on the pile, which causes the reduction of vertical effective stress and thus the skin friction, according to formula (5). The higher the drilling borehole diameter, the larger the excavation produced. Consequently, the skin friction decreases with the increasing drilling borehole diameter, as shown in Figure 8.

The skin friction values are decreasing to negative values along with the depth of the mucky clay zone. Overall, the skin friction decreases with the increase of diameter within the depth of the neutral point, while it increases with the increase of diameter beyond the neutral depth. When the buried depth is 22.0 m, the negative friction reaches maximum of −13.91 kPa. Then, the skin friction increases rapidly.

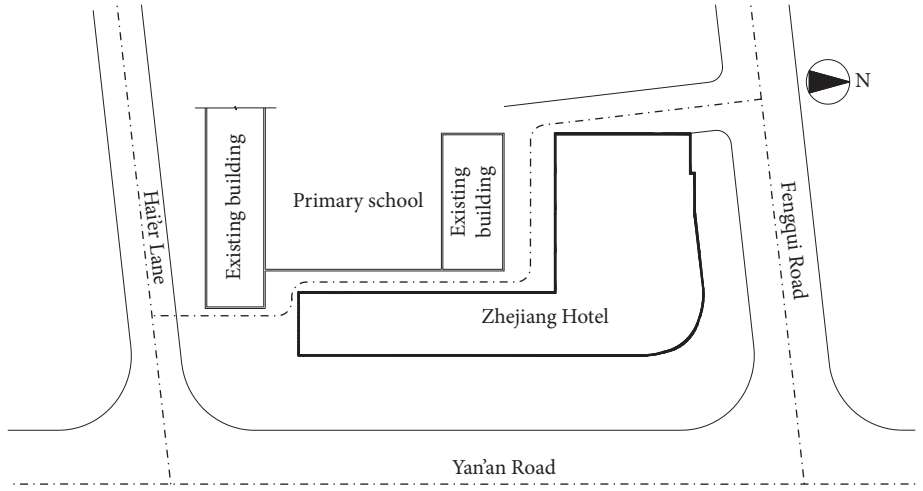

Figure 7: The layout of Zhejiang Hotel.

Table 1: Physical and mechanical parameters of soil.

Layer number	Name of soil layer	t (m)	γ (kN/m^3)	c (kPa)	φ (°)	E_s (MPa)	μ	$N_{63.5}$ values
①$_2$	Plain fill	5.1	17.7	9.0	12.0	20.0	0.35	
③$_2$	Mucky silty clay	11.5	17.9	11.2	19.5	17.5	0.35	
③$_3$	Mucky clay	6.0	17.1	19.6	7.0	15.0	0.35	
④$_3$	Clay	5.0	19.0	37.0	14.5	36.5	0.35	55
⑤	Silty clay	5.0	18.9	35.0	16.0	35.0	0.35	
⑥$_1$	Clay	5.4	18.0	52.5	9.0	22.5	0.35	
⑧$_1$	Highly weathered andesite	—	22.0	450	53	150.0	0.25	

Note. t is the thickness of soil layer; γ is the unit weight of soil layer; c and φ are the cohesive and internal friction angle, respectively; E_s is the compression modulus; μ is Poisson's ratio; $N_{63.5}$ values are the blow counts received from the heavy dynamic penetration test.

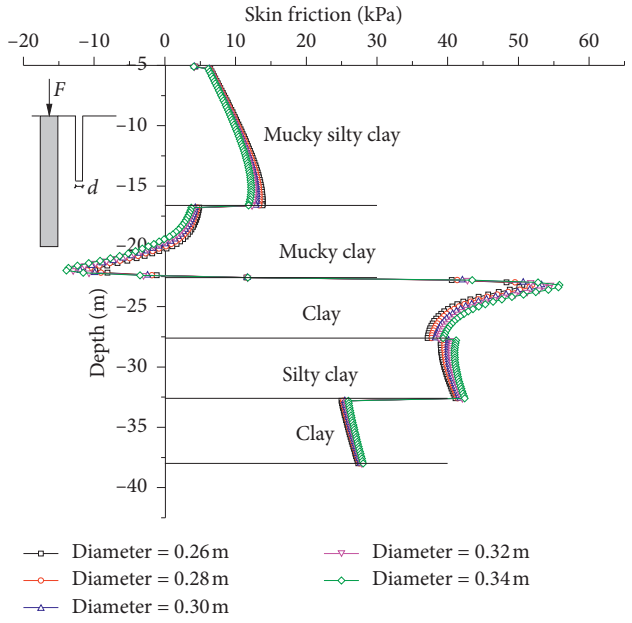

Figure 8: Variations of skin friction of the existing foundation pile at different segments under the impact of different borehole diameters.

The influence of borehole diameter on the skin friction of the existing pile becomes smaller and smaller within the clay, silty clay, and clay.

Table 2: Effect of borehole diameter on the end resistance of the existing foundation pile.

Diameter (m)	0.26	0.28	0.30	0.32	0.34
R_d	0.9701	0.9675	0.9650	0.9626	0.9601
Decreasing percentage	—	−0.3	−0.5	−0.8	−1.0

Table 2 shows the influence of borehole diameter on the end resistance of the existing pile. This influence is indicated by the R_d value, which is the ratio of end resistance with different borehole diameters to the end resistance of the existing pile when it has not been drilled. It shows that the R_d value decreases very slowly with the increase of borehole diameters; thus, the borehole diameter is insensitive to the end resistance of the existing pile. Note that the average overburden load in ground h_m changes with the excavation, causing the variation of vertical stress σ_v, and thus the stress component σ_v in the plane direction that represents boundary 1 (t_1) and the one that runs perpendicular to it (s_1) change. However, their consequent effect on the end resistance due to the variation of borehole diameter is negligible.

1.4.2. Depth of Drilling Borehole. During an excavation, stress relief could occur; the bearing behavior of the existing pile could be impacted. Figure 9 and Table 3 show the influence of depth of borehole on the skin friction and end

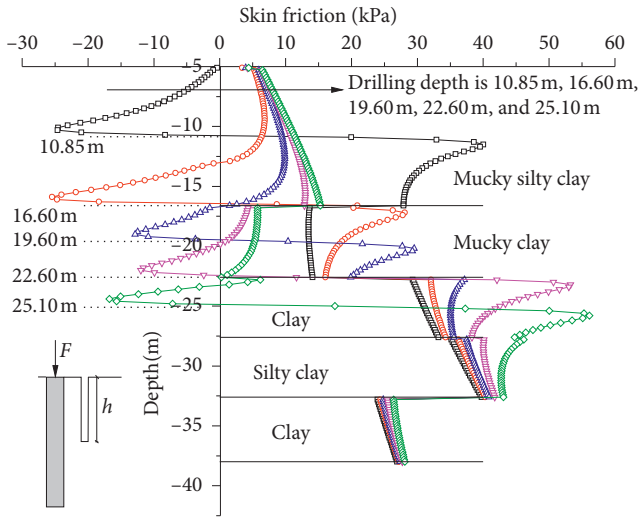

Figure 9: Effect of depth of drilling borehole on the skin friction of the existing foundation pile.

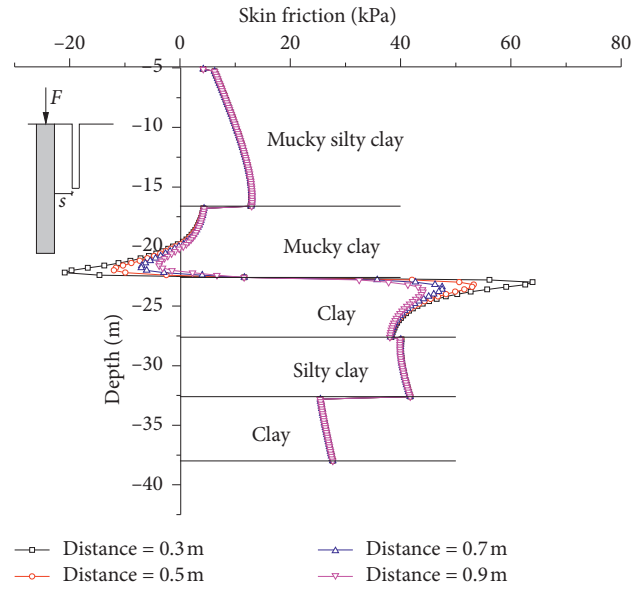

Figure 10: Effect of distance of drilling borehole on the skin friction of the existing foundation pile.

Table 3: Effect of depth of drilling borehole on the end resistance of the existing foundation pile.

Depth (m)	10.85	16.6	19.6	22.6	25.1	27.6
R_h	0.9758	0.9724	0.9694	0.9652	0.9599	0.9519
Decreasing percentage	—	−0.3	−0.7	−1.1	−1.6	−2.4

resistance of the existing pile, respectively. The diameter of borehole is 0.3 m, and the distance between existing piles is 0.5 m. The skin friction of the existing pile distributes differently within different soil layers, but the trend is similar in different soil layers, as shown in Figure 9. The skin friction increases generally with the increase of drilling depth. The influence of drilling depth on the skin friction within clay could be negligible. The results also show that the negative friction appears about 3 m above the borehole tip, except when the drilling depth is 10.85 m. The skin friction changes from negative friction to positive friction quickly near the borehole tip.

Table 3 shows the influence of depth of drilling borehole on the end resistance of the existing pile. This influence is indicated by the R_h value, which is the ratio of end resistance with different drilling depths to the end resistance of the existing pile when it has not been drilled. It shows that the R_h value decreases rather slowly with the drilling depth of borehole increasing from 10.85 m to 27.6 m. Thus, the end resistance of the existing pile is insensitive to the variation of drilling depth.

1.4.3. Distance between the Existing Foundation Pile and Drilling Borehole. The distance between the existing foundation pile and drilling borehole is a key parameter. As expected, the smaller the distance, the greater the influence of bearing behavior of the existing foundation pile. Figure 10 shows the influence of distance between the existing pile and borehole on the skin friction of the existing pile. The depth and diameter of drilling borehole are 17.5 m and 0.3 m, respectively. As shown in Figure 10, the influence could be negligible within the depth of borehole. For example, the distance of drilling borehole increases from 0.3 m to 0.9 m, and the corresponding skin frictions of the existing foundation pile at the burial depth are 10.50 kPa, 10.54 kPa, 10.54 kPa, 10.55 kPa, and 10.55 kPa, respectively. The negative skin friction would appear below 2.3–4.9 m of borehole tip. As the distance increases, the extreme point decreases to some extent. This phenomenon also occurs in the clay. Generally, the influence curves of distance on skin friction of the existing foundation pile are coincident but negligible.

Table 4 shows the influence of distance of drilling hole on the end resistance of the existing foundation pile. This influence is indicated by R_s, which is the ratio of end resistance with different distances to the end resistance of the existing pile when it has not been drilled. It shows that R_s increases slowly with the increase of distance, but the increment is rather small.

1.4.4. Number of Boreholes. During the underpinning construction, each pile cap is connecting with several underpinning piles. Thus, the number of boreholes is also an important parameter. In this section, the number of boreholes is analyzed as shown in Figure 11 and Table 5. The depth and distance of borehole are 17.5 m and 0.5 m, respectively. The results show that the skin friction of the existing foundation pile decreases rapidly with number of boreholes from one to four within the mucky silty clay. For example, the skin friction around mucky silty clay is positive when there are one or two boreholes; the negative skin friction occurs when there are three boreholes; the negative skin friction reaches the minimum value when there are four boreholes. The tendency of skin friction around the mucky clay is like the mucky silty clay. However, the skin friction

Table 4: Effect of distance of drilling borehole on the end resistance of the existing foundation pile.

Distance (m)	0.3	0.5	0.7	0.9
R_s	0.9651	0.9652	0.9652	0.9653
Decreasing percentage	—	0.01	0.01	0.02

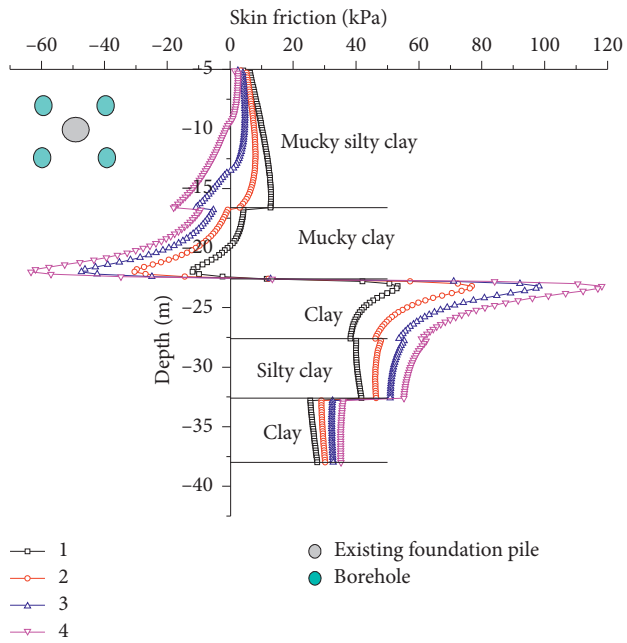

Figure 11: Effect of number of boreholes on the skin friction of the existing foundation pile.

Table 5: Effect of number of boreholes on the end resistance of the existing foundation pile.

Number	1	2	3	4
R_n	0.9650	0.9650	0.9650	0.9650
Decreasing percentage	—	0	0	0

around the clay becomes positive and its value decreases with the increase of depth, while it increases with the increasing number of boreholes. The reason may be that the number of boreholes would influence the vertical effective stress, causing changes in skin friction.

Table 5 shows the influence of number of boreholes on the end resistance of the existing foundation pile. This influence is indicted by R_n, which is the ratio of end resistance with different number of boreholes to the end resistance of the existing pile when it has not been drilled. The ratio of end resistance is 0.9650 regardless of borehole number. Thus, there is no influence of number of boreholes on the ratio of end resistance.

To summarize, all the parameters including borehole diameter, depth of drilling borehole, distance between the existing foundation pile and drilling borehole, and number of boreholes have a negligible impact on the end resistance. This is expected according to our derivation for theoretical formulas of the end resistance. The details can be found from formulas (10) to (34). However, different patterns were found regarding the effect of different parameters on the skin friction of the existing foundation pile, and the influence extent for different parameters is also different. Among the four parameters, the borehole diameter and the pile-pile distance have much lower impact on the skin friction of the existing foundation pile compared to the depth of drilling borehole and number of boreholes. This result indicates that the depth of drilling borehole and number of boreholes should be considered in the design of the proposed excavation scheme. For example, the sensitivity analysis of these two parameters should be performed to optimize the excavation design. We also found that the drilling parameters could have opposite impacts on the skin friction of existing piles. For example, in the upper soil layers, as the number and diameter of boreholes increase, the skin friction decreases, while in the lower soil layers, the skin friction increases with the number and diameter of boreholes.

Our study shows that the new excavation technique produces a reasonable result of bearing behavior of existing foundation piles regarding skin friction and end resistance in the case study. The parameter analysis could contribute to the understanding of key parameters (the depth of drilling borehole and the number of boreholes) and their value range during the excavation process. These parameters could thus be used as design ones in the engineering design work. As the Zhejiang Hotel project is still under planning stage, our new excavation scheme has not been verified in real engineering projects. Future reports will be issued once the project is completed after using the proposed excavation technique.

2. Conclusions

Given the excavation technique is still under development for high-rise buildings in downtown, this paper proposed a new excavation scheme that satisfies the limited construction space. By implementing the excavation, the underpinning piles are installed and connected to the cap of existing foundation piles. A case study (the Zhejiang Hotel project) was performed to illustrate the effectiveness of this excavation scheme. Also, a parameter analysis was conducted to investigate the influence of underpinning construction on the bearing behavior of existing foundation piles regarding the skin friction and end resistance of existing foundation piles.

The case study results conclude that the influence of borehole diameter, depth of drilling borehole, distance between the existing foundation pile and drilling borehole, and number of boreholes on the end resistance could be negligible. The skin friction of the existing pile decreases with the increase of the number and diameter of borehole in the upper soil layers. However, it increases with the number and diameter of borehole in the lower soil layers. The influence of borehole diameter and the distance between the existing pile and borehole on the skin friction could be ignored, while the depth of drilling borehole and the number of boreholes should be considered in the design of the

proposed excavation scheme. The proposed new excavation technique could be potentially used for real engineering design of underneath excavation projects for high-rise buildings in downtown.

Data Availability

The data used to support the findings of this study are available from the corresponding author upon request.

Conflicts of Interest

The authors declare that there are no conflicts of interest regarding the publication of this paper.

Acknowledgments

This study was supported by the Zhejiang Natural Science Foundation Exploration Project (grant no. LQ20E080010), Postdoctoral Science Foundation of Zhejiang Province (grant no. zj20180081), General Industrial Projects of Taizhou Science and Technology Bureau (grant no. 1801gy22), and Taizhou University Training Project (grant no. 2017PY004).

References

[1] G. S. William, M. W. Elin, and C. Patrick Koelling, *Engineering Economy*, Prentice Hall, Englewood, Co, USA, 2015.

[2] C. H. Qiu, Y. Q. Zhan, Y. K. Qin, and S. G. Pi, "Structural design for renovation and extension of Beijing music hall," *Building Science*, vol. 15, no. 6, pp. 311–320, 1999.

[3] Y. W. Wen, S. Y. Liu, M. L. Hu, and G. S. Zhang, "Deformation control techniques for existing building during construction process of basement," *Chinese Journal of Geotechnical Engineering*, vol. 35, no. 10, pp. 1914–1921, 2013.

[4] B. Simpson and P. J. Vardanega, "Results of monitoring at the British Library excavation," *Geotechnical Engineering*, vol. 167, no. GE2, pp. 99–116, 2013.

[5] H. F. Shan, F. Yu, T. D. Xia, C. G. Lin, and J. L. Pan, "Performance of the underpinning piles for basement-supplementing retrofit of a constructed building," *Journal of Performance of Constructed Facilities*, vol. 31, no. 4, pp. 1–10, 2017.

[6] H. G. Poulos and L. T. Chen, "Pile response due to unsupported excavation-induced lateral soil movement," *Canadian Geotechnical Journal*, vol. 33, no. 4, pp. 670–677, 1996.

[7] H. G. Poulos and L. T. Chen, "Pile response due to excavation-induced lateral soil movement," *Journal of Geotechnical and Geoenvironmental Engineering*, vol. 123, no. 2, pp. 94–99, 1997.

[8] C. F. Leung, Y. K. Chow, and R. F. Shen, "Behavior of pile subject to excavation-induced soil movement," *Journal of Geotechnical and Geoenvironmental Engineering*, vol. 126, no. 11, pp. 947–954, 2000.

[9] D. E. Ong, C. E. Leung, and Y. K. Chow, "Pile behavior due to excavation-induced soil movement in clay. I: stable wall," *Journal of Geotechnical and Geoenvironmental Engineering*, vol. 132, no. 1, pp. 36–44, 2006.

[10] M. A. Soomro, D. A. Mangnejo, R. Bhanbhro, N. A. Memon, and M. A. Memon, "3D finite element analysis of pile responses to adjacent excavation in soft clay: effects of different excavation depths systems relative to a floating pile," *Tunnelling and Underground Space Technology*, vol. 86, pp. 138–155, 2019.

[11] C. F. Leung, J. K. Lim, R. F. Shen, and Y. K. Chow, "Behavior of pile groups subject to excavation-induced soil movement," *Journal of Geotechnical and Geoenvironmental Engineering*, vol. 129, no. 1, pp. 58–65, 2003.

[12] D. E. L. Ong, C. F. Leung, and Y. K. Chow, "Behavior of pile groups subject to excavation-induced soil movement in very soft clay," *Journal of Geotechnical and Geoenvironmental Engineering*, vol. 135, no. 10, pp. 1462–1474, 2009.

[13] F. Liang, F. Yu, and J. Han, "A simplified analytical method for response of an axially loaded pile group subjected to lateral soil movement," *KSCE Journal of Civil Engineering*, vol. 17, no. 2, pp. 368–376, 2013.

[14] R. D. Mindlin, "Force at a point in the interior of a semi-infinite solid," *Physics*, vol. 7, no. 5, pp. 195–202, 1936.

[15] Z. Y. Xu, "Calculation formula of vertical stress in foundation depends on Mindlin's formula," *Chinese Journal of Civil Engineering*, vol. 4, no. 4, pp. 485–497, 1957, in Chinese.

[16] S. J. Wang, M. Zhang, and J. Z. Zhang, "Study on the application of theory of Mindlin's stress solution," *Engineering Mechanics*, vol. 18, no. 6, pp. 141–148, 2001, in Chinese.

[17] J. Han and S.-L. Ye, "A field study on the behavior of a foundation underpinned by micropiles," *Canadian Geotechnical Journal*, vol. 43, no. 1, pp. 30–42, 2006.

[18] H. F. Shan, T. D. Xia, F. Yu, and J. H. Hu, "Critical buckling capacity of piles with different pile-head constraints for excavation beneath existing foundation," *Chinese Journal of Geotechnical Engineering*, vol. 39, no. S2, pp. 49–52, 2017, in Chinese.

[19] J. B. Burland, "Shaft friction of piles in clay—a simple fundamental approach," *Ground Engineering*, vol. 6, no. 3, pp. 30–42, 1973.

[20] D. Loukidis and R. Salgado, "Analysis of the shaft resistance of non-displacement piles in sand," *Géotechnique*, vol. 58, no. 4, pp. 283–296, 2008.

[21] R. J. Chandle, "The shaft friction of piles in cohesive soils in terms of effective stresses," *Civil Engineering and Public Works Review*, vol. 63, no. 738, pp. 48–51, 1968.

[22] L. M. Zhang, Y. Xu, and W. H. Tang, "Calibration of models for pile settlement analysis using 64 field load tests," *Canadian Geotechnical Journal*, vol. 45, no. 1, pp. 59–73, 2008.

[23] Q. Q. Zhang, S. C. Li, L. P. Li, and Y. J. Chen, "Simplified method for settlement prediction of pile groups considering skin friction softening and end resistance hardening," *Chinese Journal of Rock Mechanics and Engineering*, vol. 32, no. 3, pp. 615–624, 2013, in Chinese.

[24] X. N. Gong, C. J. Wu, F. Yu, K. Fang, and M. Yang, "Shaft resistance loss of piles due to excavation beneath existing basement," *Chinese Journal of Geotechnical Engineering*, vol. 35, no. 11, pp. 1957–1964, 2013, in Chinese.

[25] G. Zheng, S. Y. Peng, C. W. W. Ng, and Y. Diao, "Excavation effects on pile behaviour and capacity," *Canadian Geotechnical Journal*, vol. 49, no. 12, pp. 1347–1356, 2012.

[26] E. Hoek and E. T. Brown, *Underground Excavation in Rock*, The Institution of Mining and Metallurgy, London, 1980.

[27] E. Hoek and E. T. Brown, "Practical estimates of rock mass strength," *International Journal of Rock Mechanics and Mining Sciences*, vol. 34, no. 8, pp. 1165–1186, 1997.

[28] A. Serrano and C. Olalla, "Ultimate bearing capacity at the tip of a pile in rock-part 1: theory," *International Journal of Rock Mechanics and Mining Sciences*, vol. 39, no. 7, pp. 833–846, 2002.

[29] C. J. Wu, X. N. Gong, F. Yu, and Q. Q. Zhang, "Effect of excavation beneath existing buildings on loading stiffness of

piles," *Chinese Journal of Rock Mechanics and Engineering*, vol. 33, no. 8, pp. 1526–1535, 2014.

[30] A. Serrano and C. Olalla, "Ultimate bearing capacity of rock masses," *International Journal of Rock Mechanics and Mining Sciences & Geomechanics Abstracts*, vol. 31, no. 2, pp. 93–106, 1994.

[31] C. J. Wu, X. N. Gong, F. Yu, C. H. Lou, and N. W. Liu, "Pile base resistance loss for excavation beneath existing high-rise building," *Journal of Zhejiang University (Engineering Science)*, vol. 48, no. 4, pp. 671–678, 2014.

[32] *Geological Survey Report of Zhejiang Hotel Expansion Project*, Hangzhou Surveying and Mapping Institute, Hangzhou, China, 1996.